ELSEVIER

Chemical Engineering Journal 96 (2003) 125–131

Chemical Engineering Journal

www.elsevier.com/locate/cej

Effect of fluidization conditions on the membrane permeation rate in a membrane assisted fluidized bed

S.A.R.K. Deshmukh, M. van Sint Annaland*, J.A.M. Kuipers

Department of Science and Technology, Twente University, P.O. Box 217, 7500 AE Enschede, The Netherlands

Abstract

The effects of fluidization conditions on the membrane permeation rate in a membrane assisted fluidized bed (MAFB) employing micro-porous membranes have been studied experimentally in a square fluidized bed, equipped with vertical ceramic membranes positioned in a staggered arrangement. First, the morphological parameters of the membranes have been determined with separate experiments and the membrane gas permeation rates could be well described with the dusty gas model. Secondly, the effects of the fluidization conditions, such as the particle size, superficial gas velocity and freeboard pressure on the membrane permeate flow rate have been measured. The membrane permeation rates from the fluidized bed could be well described by taking into account the local pressure drop over the membrane, where the local pressure inside the fluidized bed was evaluated as the hydrostatic head using the average bed porosity.

Keywords: Membrane assisted fluidized bed; Hydrodynamics; Ceramic membranes; Dusty gas model

1. Introduction

A fluid bed membrane reactor (FBMR) is a special type of reactor that combines the advantages of a fluidized bed and a membrane reactor. Despite the excellent heat transfer properties of a fluidized bed axial gas back-mixing can considerably decrease the overall reactant conversion and product selectivity. By insertion of membranes in the fluidized bed, either perm-selective or porous membranes, large improvements in conversion and selectivity can be achieved.

Firstly, the product selectivity can be increased via optimization of the axial concentration profiles via distributive feeding of one of the reactants (e.g. controlled dozing of oxygen for partial oxidation reactions) or selective withdrawal of one of the products (e.g. selective removal of hydrogen in dehydrogenation reactions). Furthermore, controlled dozing of oxygen could be used to achieve high conversions and still avoid the formation of explosive reaction mixtures, rendering the reactor inherently safe.

Secondly, the insertion of membranes decreases the effective axial dispersion via compartmentalization of the fluidized bed. Insertion of membrane bundles in a suitable configuration impedes bubble growth and macroscopic circulation patterns in the fluidized bed, thereby reducing reactant by-pass via rapidly rising large bubbles. Furthermore, gas withdrawal through the membranes decreases the superficial gas velocities in the top section of the bed, resulting in smaller gas bubbles, which increases the inter-phase gas exchange favoring high conversions [1]. Both vertical and horizontal inserts (membranes and heat transfer tubes) can be used to effectively retard the emulsion circulation and increase the bubble breakage. For the controlled dozing of one of the reactants a horizontal arrangement of inserts is usually preferred to directly control the local concentrations. For the removal of one of the intermediate products vertical membrane bundles might suffice, which are much easier to be integrated in the reactor.

The application of FBMRs to reactions of industrial importance has been investigated in the recent past. Adris et al. demonstrated both by experiments [2] and by modeling [3] that for the steam reforming of natural gas the in situ separation and removal of hydrogen via perm-selective thin-walled palladium-based membranes shifted the conventional thermodynamic equilibrium and increased the synthesis gas yields in comparison to the industrial fixed bed steam reformer. Using simulations Abdalla and Elnashaie [4] showed for the catalytic dehydrogenation of ethyl benzene to styrene and Ostrowski et al. [5] for the catalytic partial oxidation of methane to synthesis gas that with FBMRs higher product selectivities could be realized compared to fixed bed reactors. In these studies the insertion of perm-selective hydrogen membranes in the fluidized bed was investigated.

* Corresponding author. Tel.: +31-534894478; fax: +31-534892882.
E-mail address: m.vansintannaland@ct.utwente.nl
(M. van Sint Annaland).

1385-8947/$ – see front matter © 2003 Elsevier B.V. All rights reserved.
doi:10.1016/j.cej.2003.08.012

Nomenclature

B_0	membrane morphology parameter for viscous flow (m^2)
d_p	particle diameter (m)
D	gas diffusivity ($m^2\,s^{-1}$)
g	gravitational acceleration ($m\,s^{-2}$)
H_f	actual fluidization bed height (m)
H_{mf}	minimum fluidization bed height (m)
K_0	membrane morphology parameter for Knudsen flow (m)
N	molar gas flux through the membrane ($mol\,m^{-2}\,s^{-1}$)
P	pressure (Pa)
P_{av}	arithmetic mean of the pressure inside the membrane and the bed pressure (Pa)
P_{fb}	freeboard pressure (Pa)
P_0	fluid bed pressure (Pa)
ΔP	pressure drop across the membrane in the fluidized bed (Pa)
T	bed temperature (K)
u_{mf}	minimum fluidization velocity ($m\,s^{-1}$)
u_0	superficial gas velocity ($m\,s^{-1}$)
z	axial position (m)

Greek symbols

ε_e	voidage in the emulsion phase (–)
ε_{mf}	bed voidage at minimum fluidization conditions (–)
μ_g	gas viscosity (Pa s)
ν_M	mean molecular velocity of gas ($m\,s^{-1}$)
ρ_g	gas density ($kg\,m^{-3}$)
ρ_p	particle density ($kg\,m^{-3}$)
τ	membrane pore tortuosity (–)
ϕ	molar flow of gas through the membrane

This work focuses on the application of porous membranes, e.g. for the controlled dozing of oxygen in a fluidized bed for the partial oxidation of methanol to formaldehyde. It is investigated experimentally whether the fluidization conditions, such as particle size, superficial gas velocity and freeboard pressure influence the permeation rates through the porous membranes. First, the experimental set-up for the membrane assisted fluidized bed (MAFB) is shortly described. Subsequently, the membrane morphology parameters are determined from separate experiments. And finally, the influence of the fluidization conditions on the permeate fluxes are discussed and modeled.

2. Experimental

In a fluidized bed with a square cross-section (0.15 m × 0.15 m × 0.95 m) constructed from lexan 39 ceramic membrane tubes (1.5 mm inner diameter, 2.5 mm outer diameter, length 0.15 m and average pore size 0.15 μm) were positioned vertically with an equilateral pitch of 0.02 m (see Fig. 1). The fluidized bed was filled with glass beads ($2550\,kg\,m^{-3}$) and fluidized with air at ambient temperature via a porous plate distributor (with a pore size of about 10 μm). At the outlet a filter was placed to avoid carry-over of the fines. The freeboard pressure was controlled by passing the outlet gas through a water column. By maintaining atmospheric pressure at the permeate side of the membranes, gas was removed from the fluidized bed and the membrane permeate flow was measured with a Brooks mass flow meter. To investigate the influence of the fluidized bed hydrodynamic behavior on the membrane permeate flow, the permeate flow was measured at different superficial gas velocities and freeboard pressures for Geldart A and B type particles (see Table 1).

2.1. Permeability measurements to determine the membrane morphology parameters

Gas permeation through micro-porous inorganic membranes can in general be attributed to Knudsen diffusion, viscous flow and bulk diffusion mechanisms. To simplify the interpretation of the experimental results, the experiments were carried out without concentration gradients, so that the contribution due to bulk diffusion could be ignored in this work. Furthermore, as a rule of thumb, Knudsen diffusion dominates when the mean free path is larger than 10 times the pore diameter [7]. Since the estimated mean free path for air (90 nm) is in the same order of magnitude as the pore radius of the membrane (75 nm), both the Knudsen diffusion and viscous flow will contribute to the total gas flux through the membrane, which can be described by the dusty gas model according to

$$N = -\frac{1}{RT}\left[K_0 \nu_M + B_0 \frac{P}{\mu}\right] \nabla P \tag{1}$$

where N represents the molar gas flux, R the universal gas constant, T temperature; μ the gas viscosity and P and ∇P the pressure and pressure gradient. The mean molecular velocity can be calculated with

$$\nu_M = \sqrt{\frac{8RT}{\pi M}} \tag{2}$$

where M is the average molar mass of air.

Table 1
Different particles used in the experiments with their operating conditions calculated from Kunii and Levenspiel [6]

Experiment	Geldart classification	Particle size (μm)	u_{mf} ($m\,s^{-1}$)	ε_{mf} (–)
I	A	40–70	0.00439	0.454
II	B	80–110	0.0121	0.434
III	B	150–180	0.0327	0.418
IV	B	230–320	0.0905	0.398

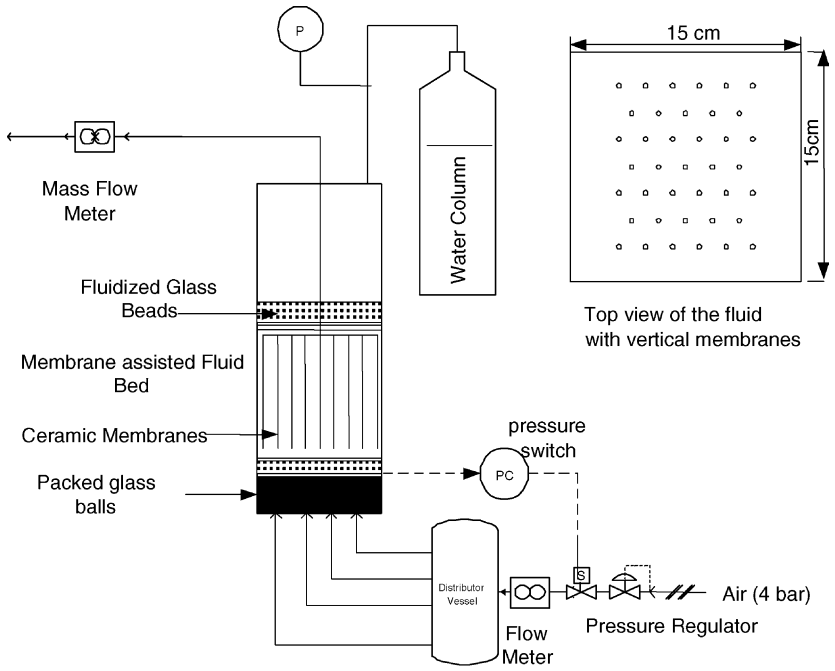

Fig. 1. Schematic diagram of the experimental set-up for the gas permeation measurements in the MAFB: (a) side view; (b) top view.

The Knudsen diffusion and viscous flow morphology parameters, K_0 and B_0, respectively, are membrane-specific constants and independent of the permeating gas, provided that no other gas–membrane interaction takes place than collision (e.g. no dissolution, adsorption or surface diffusion). For homogeneous membranes with cylindrical pores K_0 and B_0 can be calculated with

$$K_0 = \frac{2\varepsilon r_p}{3\tau} \quad \text{and} \quad B_0 = \frac{\varepsilon r_p^2}{8\tau} \tag{3}$$

where ε is the membrane porosity, τ the membrane tortuosity and r_p the pore radius.

Since real membranes have very complex structures, K_0 and B_0 must be determined experimentally. Integrating Eq. (1) over a tubular membrane wall using that the gas permeate flow ($N{\cdot}r$) is constant results in

$$N_o = \frac{1}{RT}\left[K_0 \nu_M + B_0 \frac{P_{av}}{\mu_g}\right] \frac{\Delta P}{r_o \ln(r_o/r_i)} \tag{4}$$

where N_o is the molar gas flux at the outer membrane area, P_{av} the arithmetic mean of the gas pressure at both sides of the membrane, ΔP the total pressure difference over the membrane and r_i and r_o the inner and outer membrane radii, respectively. Plotting $N_o RTr_o \ln(r_o/r_i)/(\Delta P \nu_M)$ versus P_{av}/ν_M in graph will give K_0 as the intercept and B_0 as the slope.

The membrane morphology parameters were determined in a separate experimental set-up (see Fig. 2). Using a

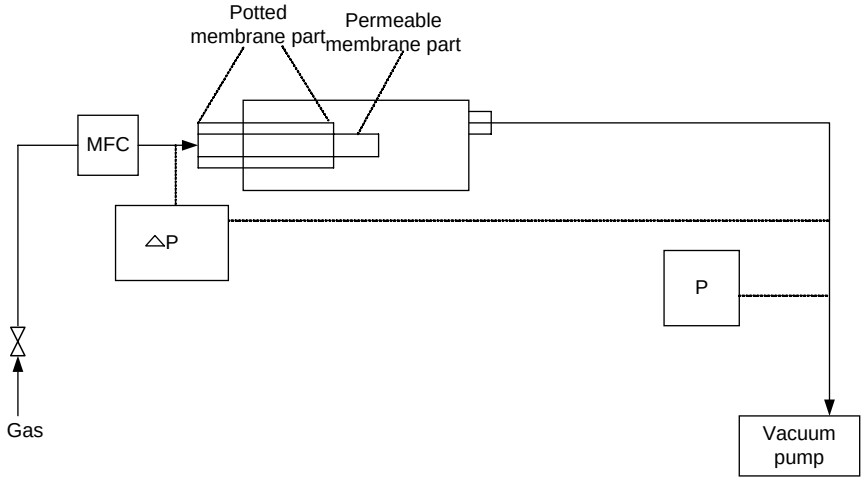

Fig. 2. Schematic diagram of the experimental set-up to determine the membrane morphology parameters.

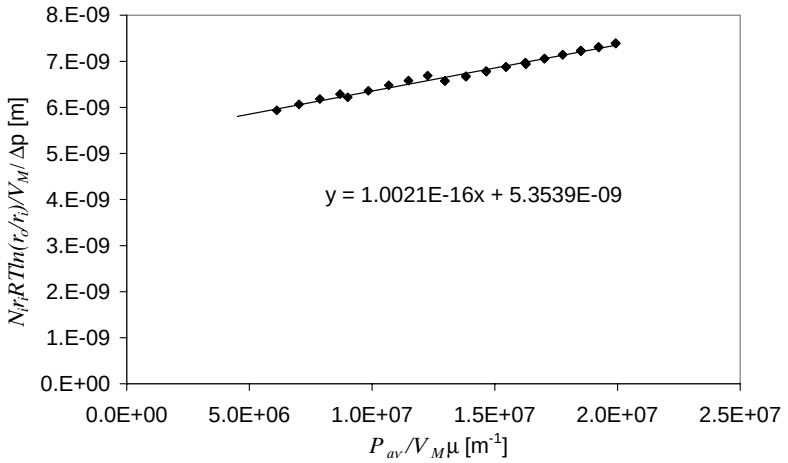

Fig. 3. Determination of the membrane morphology parameters from the experiments.

dead-end membrane construction a controlled flow of N_2 was forced through the membrane and the resulting pressure drop was measured via pressure transducers (see for further details on the experimental technique [8]). By blocking part of the membrane surface it was ensured that the axial pressure drop in the membrane tube was negligibly small, which was confirmed by constant values of K_0 and B_0. For the ceramic tubes the experimentally determined values for B_0 and K_0 are 1.00×10^{-16} m^2 and 5.35×10^{-9} m, respectively (see Fig. 3). With these values for B_0 and K_0 and assuming cylindrical pores, a pore radius of 100 nm can be estimated (using Eq. (3)), which compares reasonably with the actual pore radii (75 nm).

2.2. Effect of fluidization conditions on the membrane permeate flow

In order to study the effect of the operating conditions in the fluidized bed on the permeate flow through the porous membranes, the membrane permeate flow was measured at different superficial gas velocities and different freeboard pressures for powders with different particle size ranges. The overall effect of the superficial gas velocity on the total permeate flow is shown in Fig. 4, while the effect of the particle size is given in Fig. 5. The figures clearly show that there is hardly any overall effect of both the superficial gas velocity and the particle size on the permeate flow at the same freeboard pressure. Small deviations in the membrane permeation at high superficial gas velocities can be attributed to the plugging of the filter placed at the exit of the fluid bed by fine particles, which increases the freeboard pressure slightly.

3. Modeling of membrane gas permeation in an MAFB

The experimental results have shown that the superficial gas velocity and the particle size in the fluidized bed have no overall effect on the gas permeation through the ceramic membrane tubes, indicating that the solids circulation patterns and the local bubble fraction do not influence the overall gas permeation fluxes. Moreover, from the experiments it can be concluded that only the freeboard pressure determines the overall gas permeation flow rate for the same type of solids and provided that concentration gradients are absent.

The local gas permeation rate is apparently only determined by the local pressure drop across the membrane. The local pressure in the fluidized bed, P_0, at a vertical distance z from the distributor, can be estimated with the freeboard pressure, P_{fb}, augmented with the hydrostatic head of the bed:

$$P_0 = P_{\mathrm{fb}} + (H_{\mathrm{f}} - z)(1 - \varepsilon_{\mathrm{bed}})(\rho_{\mathrm{p}} - \rho_{\mathrm{g}})g \tag{5}$$

where H_{f} represents the total bed height and $\varepsilon_{\mathrm{bed}}$ the average bed porosity. The average bed porosity was taken here, since the bed porosity hardly changes as a function of height [9].

The local permeate flow ϕ through a single vertical membrane tube varies as a function of the axial position z in the bed according to

$$\frac{\mathrm{d}\phi}{\mathrm{d}z} = 2\pi(N \cdot r)_{\mathrm{i}} = \frac{2\pi}{RT\ln(r_{\mathrm{i}}/r_{\mathrm{o}})}\left[K_0\nu_{\mathrm{M}}(P_{\mathrm{o}} - P_{\mathrm{i}}) + \frac{B_0}{2\mu_{\mathrm{g}}}(P_{\mathrm{o}}^2 - P_{\mathrm{i}}^2)\right] \tag{6}$$

where P_{o} and P_{i} represent the local pressures at outside and inside the membrane tube. The total gas flow permeated through a single vertical membrane tube can then be obtained via substitution of Eq. (5) into Eq. (6) and integration over the bed height. The average bed porosity varies considerably for different particle sizes and superficial gas velocities. However, the product of the expanded bed height and the average solid porosity, and hence the total permeation flow, remained practically unaltered in the experiments, since the initial packed bed height was kept constant.

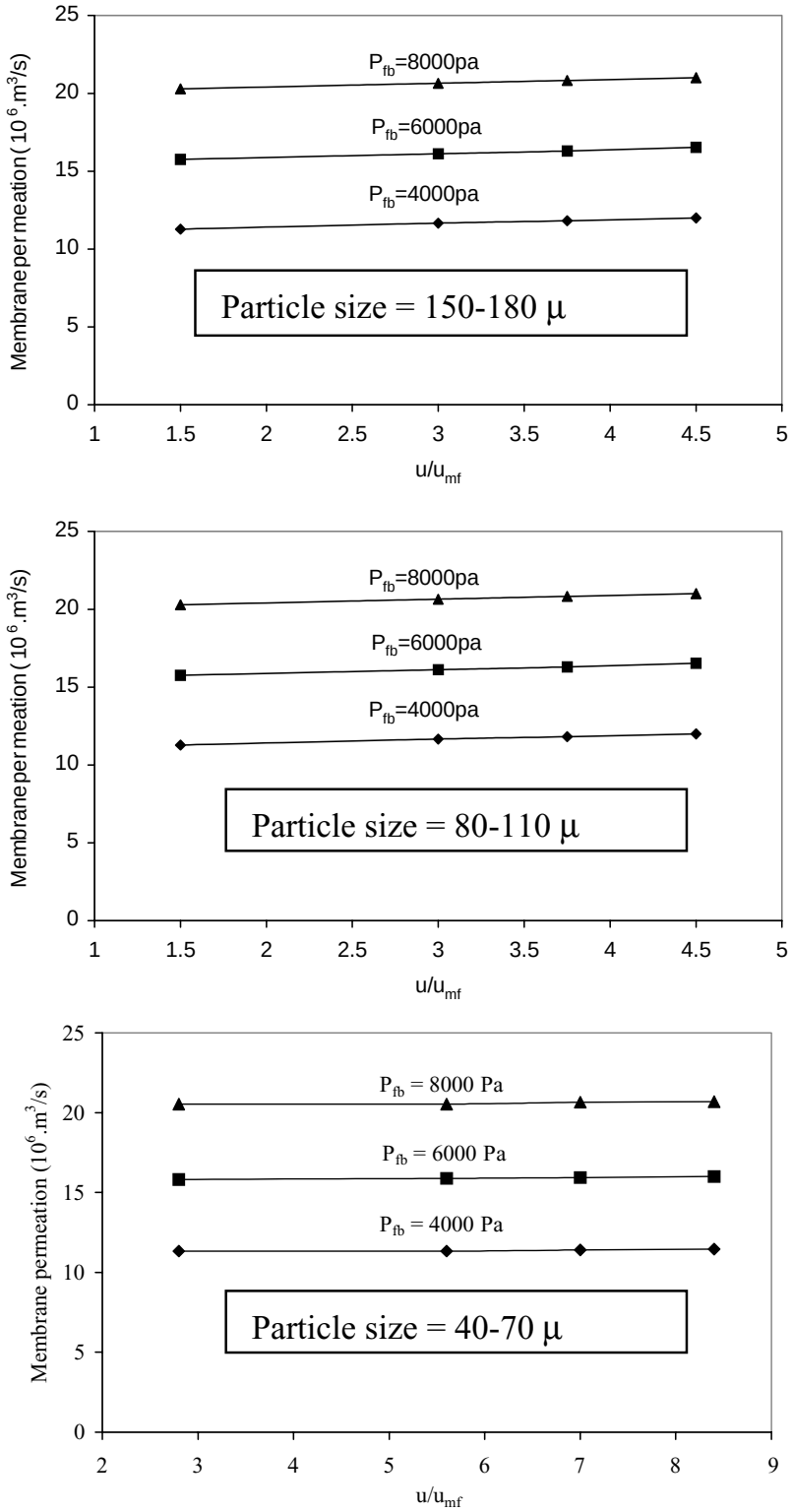

Fig. 4. Effect of the relative superficial gas velocity (u/u_{mf}) and freeboard pressure (P_{fb}) on the measured permeation rate for different particle sizes.

To compare the results between the theoretically calculated permeate flow rate and the measured permeate flow rate, all the data points in this study are plotted as a parity plot in Fig. 6. This plot shows that the experimentally determined and theoretically calculated membrane permeate flow rates match closely and that the deviation is less than 6%. This also shows that the method used to obtain the membrane morphology parameters was correct and gave

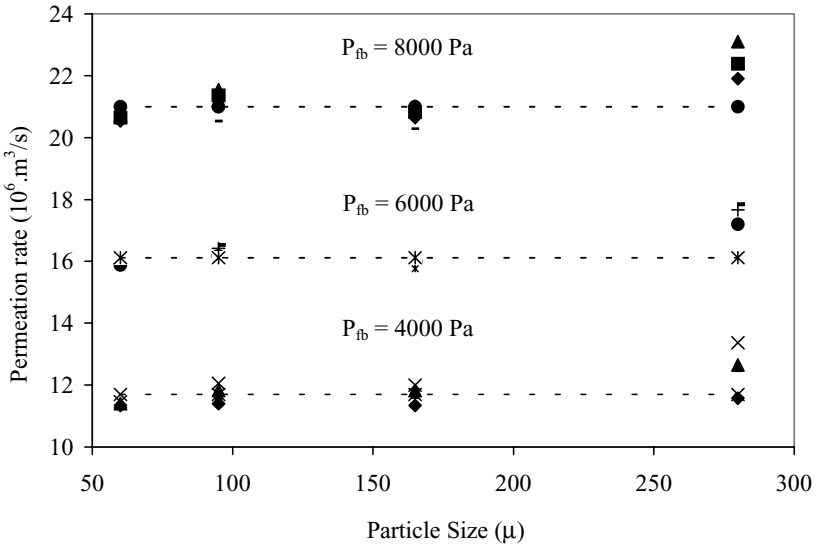

Fig. 5. Effect of particle size on the membrane permeation rate at different relative superficial gas velocities (u/u_{mf}) and freeboard pressures (P_{fb}).

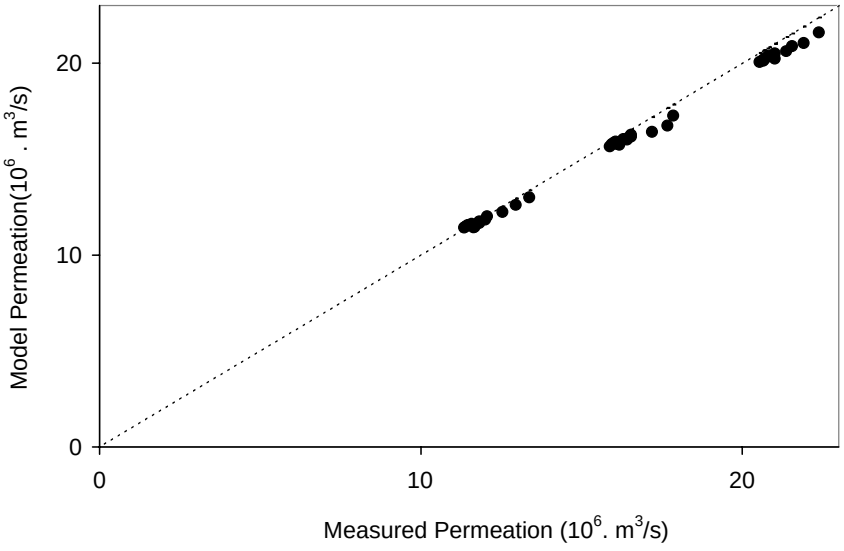

Fig. 6. Parity plot for the experimentally determined and theoretically calculated membrane permeation rates.

accurate measurements of the membrane properties within an experimental error of 10% and 6% for B_0 and K_0, respectively.

4. Conclusions

The effect of fluidization conditions, viz. the superficial gas velocity, particle size and freeboard pressure on the gas permeation rate through porous ceramic membranes has been studied experimentally. The gas withdrawal through the membranes increased with an increase in the freeboard pressure, which could be well described by the dusty gas model where it was simply assumed that the membrane permeate flux was only a function of the local pressure in the fluidized bed, for which the hydrostatic head with the average bed porosity was taken. The superficial gas velocity as well as the particle size had no overall effect on the total amount of gas permeated through the membranes, which can be explained by the fact that the decrease in the average bed porosity at lower superficial gas velocities or larger particle sizes is counterbalanced by an increase in the bed height. Although concentration gradients in the fluidized bed and the membranes were absent in this work, this can be easily included in the dusty gas model. Moreover, since the solids circulation patterns do not affect the membrane permeation fluxes, no effects of the arrangement and pitch of the vertical membrane bundles are expected.

The membrane permeate flux expression can be directly incorporated into fluidized bed rector models, such as the

two phase bubbling bed model by Kunii and Levenspiel [6] or the improved bubble-assemblage model (BAM) of Shiau and Lin [9], which is based on the model of Kato and Wen [10], in order to model the performance of fluidized bed membrane reactors. However, in these models the effect of the membrane bundles on the gas back-mixing behavior and the heat transfer properties of submerged heat transfer tubes are not yet incorporated and additional experimental and modeling work on this subject is currently being carried out.

Acknowledgements

This research is part of the research program carried out within the Center for Separation Technology, a cooperation between the University of Twente and TNO, The Netherlands Organization for Applied Scientific Research.

References

[1] L. Mleczko, T. Ostrowski, T. Wurzel, A fluidized bed membrane reactor for the catalytic partial oxidation of methane to synthesis gas, Chem. Eng. Sci. 51 (1996) 3187.

[2] A.M. Adris, C.J. Lim, J.R. Grace, The fluid bed membrane reactor system: a pilot scale experimental study, Chem. Eng. Sci. 49 (1994) 5833.

[3] A.M. Adris, S.S.E.H. Elnashaie, R. Hughes, A fluidized bed reactor for steam reforming of methane, The Can. J. Chem. Eng. 69 (1991) 1061.

[4] B.K. Abdalla, S.S.E.H. Elnashaie, Fluidized bed reactor without and with selective membranes for the catalytic dehydrogenation of ethylbenzene to styrene, J. Membr. Sci. 101 (1995) 31.

[5] T. Ostrowski, A. Giroir-Fendler, C. Mirodatos, L. Mleczko, Comparative study of the catalytic partial oxidation of methane to synthesis gas in fixed bed and fluidized bed membrane reactors. Part II. Development of membranes and catalytic measurements, Catal. Today 40 (1998) 191.

[6] D. Kunii, O. Levenspiel, Fluidization Engineering, Butterworths, London, 1991.

[7] J. Smid, C.G. Avci, V. Gunay, R.A. Terpstra, J.P.G.M. Van Eijk, Preparation and characterization of microporous ceramic hollow fiber membranes, J. Membr. Sci. 112 (1996) 85.

[8] C.M. Guijt, I.G. Racz, T. Reith, A.B. de Haan, Determination of membrane properties for use in the modelling of a membrane distillation module, Desalination 132 (2000) 255.

[9] C. Shiau, C. Lin, An improved bubble assemblage model for fluidised bed catalytic reactors, Chem. Eng. Sci. 48 (1993) 1299.

[10] K. Kato, C. Wen, Bubble assemblage model for fluidized bed catalytic reactors, Chem. Eng. Sci. 24 (1969) 1351.